

SF-Speech: Straightened Flow for Zero-Shot Voice Clone on Small-Scale Dataset

Xuyuan Li^{†§}, Zengqiang Shang^{*†}, Hua Hua^{†§}, Peiyang Shi[†], Chen Yang^{†§},
Li Wang[†], and Pengyuan Zhang^{*†§}

[†]Laboratory of Speech and Intelligent Information Processing, Institute of Acoustics, CAS, China
Email: {lixuyuan, shangzengqiang, huahua, shipeiyang, yangchen, wangli, zhangpengyuan}@hcc1.ioa.ac.cn

[§]University of Chinese Academy of Sciences, China

Abstract—Large-scale speech generation models have achieved impressive performance in the zero-shot voice clone tasks relying on large-scale datasets. However, exploring how to achieve zero-shot voice clone with small-scale datasets is also essential. This paper proposes SF-Speech, a novel state-of-the-art voice clone model based on ordinary differential equations and contextual learning. Unlike the previous works, SF-Speech employs a multi-stage generation strategy to obtain the coarse acoustic feature and utilizes this feature to straighten the curved reverse trajectories caused by training the ordinary differential equation model with flow matching. In addition, we find the difference between the local correlations of different types of acoustic features and demonstrate the potential role of 2D convolution in modeling mel-spectrogram features. After training with less than 1000 hours of speech, SF-Speech significantly outperforms those methods based on global speaker embedding or autoregressive large language models. In particular, SF-Speech also shows a significant advantage over VoiceBox, the best-performing ordinary differential equation model, in speech intelligibility (a relative decrease of 22.4% on word error rate) and timbre similarity (a relative improvement of 5.6% on cosine distance) at a similar scale of parameters, and even keep a slight advantage when the parameters of VoiceBox are tripled. Audio samples are available at the demo page¹.

Index Terms—Speech generation, Zero-shot voice clone, Ordinary differential equation, Flow matching.

I. INTRODUCTION

Multi-speaker speech generation has been able to synthesize speech similar to human quality, benefiting from the development of neural networks. This technology has been widely applied in voice assistants, audiobooks, video dubbing, etc. As an essential branch of multi-speaker speech generation, cloning the unseen voice has attracted extensive attention. Some earlier works, like [1]–[3], utilized model adaptation to achieve this goal. These methods maintain a speaker lookup table with a finite number of speakers and enroll a new unseen speaker by fine-tuning the model with a few iterations. However, fine-tuning the model for each unseen speaker is labor-intensive and resource-intensive, and there is still a large performance gap in the voice clone task for unseen and seen speakers with these methods, especially when the unseen speakers only have a few seconds of speech.

To avoid fine-tuning models, some work maintains a hidden space containing the global speaker embedding (GSE) extracted from the reference speech. As a result, the model trained with a large number of samples from this space can deal directly with the speaker vectors of unseen speech in this hidden space. Some studies [4], [5] constructed this hidden space with a joint train speaker encoder module, while others [6], [7] chosen to build it with the help of pre-trained speaker recognition models. However, the GSE with a shape of $1 \times N$ is a bottleneck feature where the speaker information is highly compressed, making it more challenging to reconstruct the prosody and timbre of unseen speakers.

To address this problem, some other works continue or fill the reference speech with contextual learning to capture the timbre and associated prosody. Wang et al. [8]–[10] employ large language model (LLM) [11], [12] autoregressively continue the reference speech in discrete space constructed by audio codec models [13]–[15]. Recently, NaturalSpeech3 [16] constructs a discrete codec model designed to decouple speech components and continue different speech components non-autoregressively with a discrete diffusion model [17]. Although these discrete token-based methods generated speech with impressive naturalness and diversity, they rely on massive sufficient training data and yield unsatisfactory results on small-scale training data [18]. Moreover, some studies [19]–[22] show that discrete tokens exhibit lower audio reconstruction quality compared to continuous acoustic features. Apart from modeling in discrete space, some works apply contextual learning directly to the mel-spectrogram of speech. Le et al. [23], [24] trained a neural ordinary differential equation (ODE) model [25] with flow matching (FM) [26] to reconstruct the masked mel-spectrograms from random noise.

Although these ODE-based methods get an impressive result on the zero-shot voice clone in the mel-spectrograms space, it is still limited by the following two aspects: 1) The performance of ODE models trained with FM is limited by the coupling between the initial and target distributions [27], [28]. The more repetitive the coupling between the initial and target data, the greater the trajectory curvature of reverse flow learned by the ODE model, which reduces the inference efficiency and the quality of the generated speech. 2) Most current works

* Corresponding author.

¹[Online] Available: <https://lixuyuan102.github.io/Demo/>

model different acoustic features using the same network structure. However, signal features such as mel-spectrogram and latent features encoded by neural models are generated by very different processes. This implies that the network structure used by the current ODE models may not be the best for the mel-spectrogram.

This paper proposes a novel zero-shot voice clone model based on ODE trained with FM. The proposed model aims to improve the generated speech by learning **Straighter** reverse **Flow** trajectories, named SF-Speech. SF-Speech follows the previous models [23], [24], generating masked speech guided by text and contextual audio. Significantly different from previous works, SF-Speech uses a coarse feature instead of random noise as the initial distribution of ODE to generate the masked speech. The generation of coarse features is divided into two steps, in which we designed a text encoder to predict content and content-related prosody information from the content text and a speaker adder to add speaker information and speaker-related prosody to the output of the text encoder. Since this coarse feature couples to real speech independently, it can help to straighten the trajectories of reverse flow learned by the ODE model, thus reducing generation errors.

In addition, we analyze the local space correlation of two classes of popular acoustic features: signal features and neural-coded latent features. The analysis results show that the two types of acoustic features have very different local space correlations. In particular, we find the signal features have high local correlations in the time and channel domains. This explains why previous works [29]–[32] introducing 1D convolution in the time domain can assist in the generation of mel-spectrograms. Along these lines, we introduced 2D convolution in SF-Speech in a simple form to explore whether it can play a positive role in modeling mel-spectrograms.

Since the previous works were almost based on tens of thousands of hours of speech and lacked systematic comparison of existing methods on small-scale data, we conducted our experiments on 755 hours of Chinese speech. The results in VI-A show that the ODE-based methods have significant advantages over the GSE-based method and the LLM-based method when on small-scale data. In particular, SF-Speech achieves SOTA performance in terms of sound quality and intelligibility with fewer parameters. In addition, the inference efficiency evaluations in VI-B show that SF-Speech is 5.7 times faster than VALL-E and 3.8 times faster than VoiceBox. Finally, the ablation results in VI-C suggest that the 2D convolution has the potential to assist those models based on mel-spectrograms to improve the intelligibility of their generated speech.

In summary, the main contributions of this paper include:

- We proposed SF-Speech, a novel zero-shot voice model. SF-Speech straightens the reverse trajectories of ODE trained with FM by learning an initial distribution that is independently coupled to mel-spectrograms.
- We systematically compare different classes of zero-shot voice cloning methods on small-scale speech data. The comparison results show that SF-Speech achieved a new SOTA Chinese zero-shot TTS result with faster inference and fewer parameters.

- We found that the local correlations between the different acoustic features are varied, which explains why convolution plays an important role in mel-spectrogram modeling. Moreover, we explore the potential role of 2D convolution compared to 1D convolution in mel-spectrogram generation.

II. RELATED WORK

Differential equation model: From the point of view of differential equations, diffusion models on continuous space can be categorized into stochastic differential equation (SDE) and ODE models. Recent years, the SDE model [33] trained with denoise score matching [34] have achieved stunning results in image generation [35], [36], vocoders for speech [37]–[39], and acoustic modeling [40], [41]. However, it usually requires hundreds of iterations to generate acceptable samples. Subsequent studies have reduced the inference iterations by enhancing the express capability of diffusion noise [42]–[44] or designing a new reverse solver [45], [46]. Different from the SDE model, the ODE model lacked an effective training method until FM [26] was proposed. These methods make the training of ODE models less dependent on complex ODE solvers [25]. Moreover, FM allows the ODE model to get satisfactory samples in a few inference steps without improving diffusion noise or reverse solver. Le et al. [23], [24], [47] introduced the ODE model trained with FM to speech generation and outperformed those SDE-based models. However, some studies [27], [28] found the reverse trajectory curvature of ODE trained with FM is positively correlated with the degree of intersection between forward trajectories. The more repetitive the coupling of the initial and target distributions, the greater the degree of intersection between forward trajectories and the greater the curvature of the reverse trajectories, leading to more generation errors. To address this problem, Liu et al. [28] introduced multiple rectified flows to turn the arbitrary coupling of initial and target distribution into a new independent coupling. Guo et al. [48] introduced this into speech generation. However, the cumulative error due to multiple rectifying significantly impairs the inference performance, especially as the inference steps increase. Lee et al. [27] introduced another method that reduces the trajectory curvature in one training. They employ a β -VAE [49] to get a latent distribution with independent correspondences with each attribute of images as the initial distribution. On the contrary, this paper looks for the initial distribution coupling with speech independently in real sample space.

Convolution in acoustic models: FastSpeech [29] first demonstrated that combining 1D convolution and Transformer [50] can achieve better performance on speech generation than pure Transformer networks. It suggests that adjacent frames of the mel-spectrogram are highly correlated so that 1D convolution can play a role in modeling mel-spectrograms, even though the input to its Mel Decoder is not a spectrogram but a hidden representation. After that, DelightfulTTS [31] replaced the feed-forward Transformer blocks in FastSpeech with Conformer [51] blocks, and achieved better performance. In addition, StyleTTS [32] showed that the pure 1D convolution neural network can also achieve impressive results on

mel-spectrograms modeling. On the other hand, inspired by the success of diffusion models in image generation, some diffusion-based speech generation works directly follow the network structure in image generation. GradTTS [40] used the Unet network containing 2D convolution and Linear Attention in [52]. U-DiT TTS [41] combined the Unet [52] network with DiT [53] module and found that pure Transformer-based structures lead to generated mel-spectrograms lacking coherence. VoiceBox [23] combined the 1D convolution and the Transformer block linked as Unet style in [54]. While these previous works found that both 1D and 2D convolution can help Transformer in direct or diffusion modeling of mel-spectrograms, they gave no detailed reason or comparisons between 1D and 2D convolution. In this paper, from the view of the local correlation of acoustic features, we explain intuitively and statistically why convolution works better in modeling the signal acoustic features such as mel-spectrograms. In addition, we show that adding 2D convolution to the Transformer that incorporates 1D convolution can still bring potential performance gains in the diffusion modeling of mel-spectrograms.

III. SF-SPEECH

A. ODE Model trained with Flow Matching

For a generative task, its ordinary differential modeling can be represented as follows:

$$H_{t+1} = H_t + dH_t, t \in [0, T] \quad (1)$$

where the H_0 represents the initial distribution and the H_T represents target distribution. H_t is the intermediate state of these two distributions, and its differential dH_t represents the direction of forward trajectories between them. As dH_t is uniquely determined by H_t , it can be expressed by the following equation:

$$dH_t = \mathcal{F}(H_t, t) \quad (2)$$

where $\mathcal{F}(\cdot)$ could be seen as a direction calculator. Usually, a neural network with the following aim could be employed to predict the dH_t from H_t .

$$\min_{\Theta} \int_0^t \mathbb{E} [\|\mathcal{F}(H_t, t) - \Theta(H_t, t)\|^2] dt \quad (3)$$

where $\Theta(H_t, t)$ represents the direction of the reverse trajectories estimated by the neural network. However, it is difficult to give the explicit formula of $\mathcal{F}(H_t, t)$.

Fortunately, Liu et al. [26], [28] point out that if we take a non-causal perspective, there is a non-causal intermediate state H'_t :

$$H'_t = tH_T + (1-t)H_0 \quad (4)$$

Then, a non-causal direction of forward trajectories can be written as:

$$\mathcal{F}'(H'_t, t) = dH'_t = H_T - H_0 \quad (5)$$

Replacing the causal direction with $\mathcal{F}'(H'_t, t)$ as the fitting target for $\Theta(H_t, t)$. Equation (3) could be rewritten as:

$$\min_{\Theta} \int_0^t \mathbb{E} [\|\mathcal{F}'(H'_t, t) - \Theta(H_t, t)\|^2] dt \quad (6)$$

This training method is called flow matching (FM). Because ODE is a causal model, a neural estimator trained with FM will give the causal direction of the reverse trajectories at state H_t according to the marginal probability of $\mathcal{F}'(H'_t, t)$ [28]. Fig. 1 shows the relationship between the distribution of the non-causal forward trajectories and the causal reverse trajectories predicted by the neural estimator.

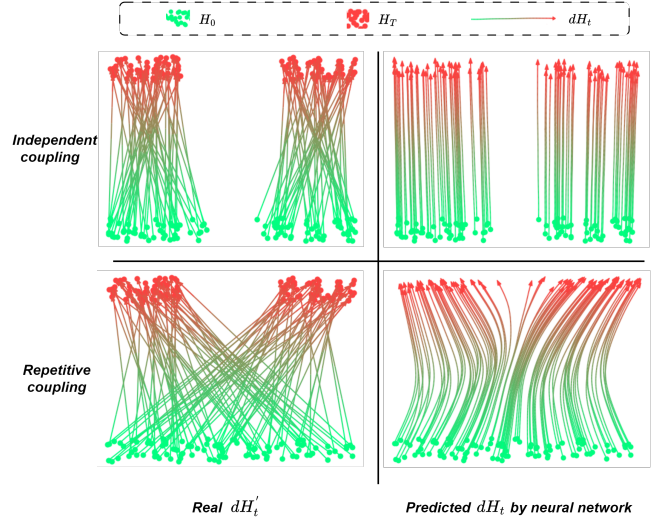


Fig. 1: Non-causal direction of forward trajectories dH'_t (left) & Causal direction of reverse trajectories dH_t (right) predicted by the neural network estimator with 128 reverse steps. The upper and lower parts show the effect of different couplings between the initial and target distributions on prediction accuracies.

While the non-causal direction of forward trajectories can assist the training of the ODE model, it also limits the ODE model if the coupling between the initial and target distributions is repetitive. Fig.1 shows the ODE model trained with FM transports different initial point distributions (green) to the same target point distribution (red). Because of the uniqueness of the solution of the ODE, the predicted reverse trajectories only fit the shape of the non-causal forward trajectories in a non-intersecting form. Consequently, the extent of intersection between non-causal forward trajectories dictates the curvature of the reverse trajectories. The predicted reverse trajectories exhibit significant curvature when the initial distribution is repetitively coupled to the target distribution, as illustrated at the bottom of Fig. 1. This excessive curvature requires more reverse steps to fit and introduces predicted errors even when the reverse steps are sufficient. For example, the green initial point on the left in the bottom-right subfigure cannot be transported to the red target point on the right, which is grossly inconsistent with the predefined coupling pairs in the bottom-left subfigure. On the contrary, if the initial distribution is independently coupled to the target distribution, as illustrated at the top of Fig. 1, the intersections between the non-causal forward trajectories are greatly reduced, and the curvature of reverse trajectories is correspondingly smaller. Since the slight curvature keeps the direction of the reverse trajectory constant, only solving a few steps can fit the entire reverse trajectory.

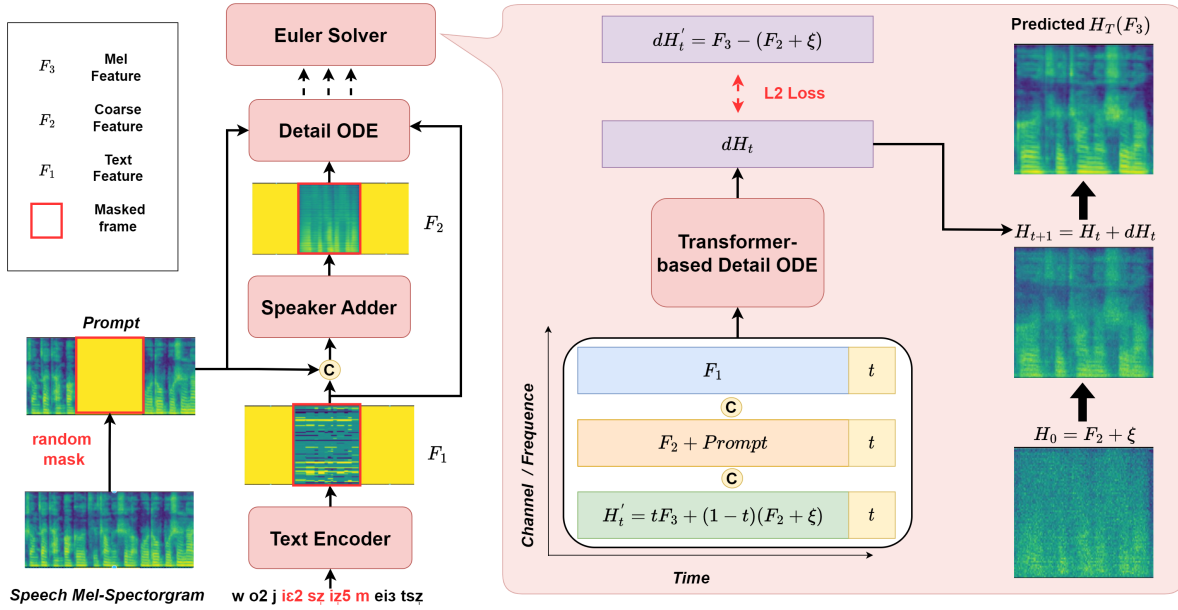


Fig. 2: Overall architecture of SF-Speech (left) and working diagram of ODE model (right) in SF-Speech.

More importantly, smaller curvature also means that the multi-step results solved by the ODE model are more consistent with the predefined coupling pairs. However, extension from 2D point to speech, as far as we know, the previous works [23], [24], [47], [48] based on ODE trained with flow matching all assume the initial data $H_0 \sim \mathcal{N}(0, I)$. This random initial noise is highly repetitively coupled to the acoustic features as the modeling target, which limits the performance of the ODE model.

B. Acoustic Model

Motivated by the need of having initial feature distributions more independently coupled to acoustic features, we assume that speech contains three main components: 1) average pronunciation, 2) text-related prosody², 3) speaker information and speaker-related prosody³. We only consider duration-independent prosody here since the phoneme duration is modeled by an additional model.

Given the above assumptions, for the same sequence of average pronunciation $X = \{x_1, x_2, \dots, x_i\}$, there are a variety of possibilities for text-related prosody. Thus, an average pronunciation sequence repetitively corresponds to different composite sequences:

$$Y \in \{X^{a_1}, X^{a_2}, \dots, X^{a_j}\} \quad (7)$$

where a_j represents the j^{th} text-related prosody scheme. Similarly, the same sequence Y could be combined with different speaker information and speaker-related prosody. The combined sequence can be written as:

$$Z \in \{Y^{b_1}, Y^{b_2}, \dots, Y^{b_n}\} \quad (8)$$

²Prosody determined only by the current and contextual text.

³Prosody changes influenced by personal information such as timbre and accent.

where b_n represents the n^{th} speaker information and related prosody. Although Z does not contain all the speech information, it represents a unique speech audio more than random noise. In other words, Z and speech are the independent coupling pair that can reduce the curvature of reverse trajectories learned by the ODE model.

To train the ODE model with this independent coupling pair data, SF-Speech generates speech through three steps, as shown in Fig. 2. First, because the average pronunciation and text-related prosody are highly correlated with the phoneme, SF-Speech models them jointly from phoneme sequences. As a result, the output of the text encoder, F_1 , represents the sequence Y in Eq. 7. Then, SF-Speech utilizes a speaker adder to extract the speaker information and speaker-related prosody from the audio context prompt and add them to the F_1 . The output of the speaker adder F_2 could be considered as the embedding of the sequence Z in Eq. 8. Finally, SF-Speech employs an ODE module, called Detail ODE, to transport F_2 to the mel-spectrograms. For convenience, we use F_3 later to represent the mel-spectrograms. To help the Detail ODE converge stably, F_1 , F_2 , and the audio context prompt are concatenated together as the input of the Detail ODE, as illustrated in the right of Fig. 2. Furthermore, to learn a continuous distribution from the limited training speech, we follow [28] and add a continuous noise ξ on F_2 when training the ODE model, where $\xi \sim \mathcal{N}(0, I)$. As a result, the optimization goal of SF-Speech can be written as:

$$\min_{\Theta} \int_0^t \mathbb{E} \left[\|dH'_t - \Theta(H'_t, F_1, F_2, \text{Prompt}, t)\|^2 \right] dt \quad (9)$$

where $H'_t = tF_3 + (1-t)\widetilde{F}_2$ and $\widetilde{F}_2 = F_2 + \xi$.

C. Text Encoder

SF-Speech splits the training audio-text pairs into the predicted part and the context prompt using a continuous mask

matrix m . The masking probability is set to 70%. Given a phoneme sequence $y_{text} \in [V]^N$ of training text, where the V means the number of phonemes appearing in the training set, a lookup table embedding it into $y_{emb} \in \mathbb{R}^{N \times H}$. Then, inspired by StyleTTS [32], a 1D convolution neural network (CNN) is employed to fuse the local features of y_{emb} and a bidirectional long-short term memory (Bi-LSTM) network follows to fuse its long-time information. A length regulator module [29] upsamples this feature to $y'_{emb} \in \mathbb{R}^{T \times H}$ with T denoting the number of mel-spectrograms frame, according to the phoneme duration. A regression duration model mentioned in [23] is trained separately to predict the masked duration with the unmasked duration and y_{text} . Finally, only the masked part $(1 - m) \odot y'_{emb}$ participate as the text feature F_1 in the subsequent data stream.

D. Speaker Adder

Since these previous methods based on context audio prompts have achieved better performance in the field of zero-shot speech synthesis compared to traditional methods based on GSE extracted by the speaker recognition model, SF-Speech extracts speaker-related information from the $Prompt = F_3 \odot m$. The speaker adder concatenates $Prompt$ with F_1 on the hidden axis as its input $z_{coa} \in \mathbb{R}^{T \times H}$. Like the text encoder, the speaker adder consists of CNN and the Bi-LSTM network. The difference is that the speaker adder utilizes the Bi-LSTM network to encode the contextual speaker information into each frame before modeling the local frames with CNN. It is worth mentioning that because our goal is to find the independent coupling distribution of mel-spectrograms in its space, the hidden dimension of the CNN network is progressively reduced until the z_{coa} is transformed into $z'_{coa} \in \mathbb{R}^{T \times C}$ with C denoting the number of frequency channels of mel-spectrograms. We found that the output of the speaker adder in the trained SF-Speech looks like a coarse mel-spectrogram, even though no mel-spectrogram-related loss constraints are made for the text and speaker adder, which is the reason why the F_2 is named as "coarse feature". Like the text feature, only the masked part $(1 - m) \odot z'_{coa}$ participate as the coarse feature F_2 in the subsequent computing.

IV. NETWORK FOR DETAIL ODE

In our experiments, we observed that employing the network lacking the convolution layer as the direction estimator of ODE-based models leads to generated mel-spectrograms lacking coherence, which also was observed in U-Dit TTS [41], which is based on the SDE model. Interestingly, we also found that using the same network and ODE modeling approach on neural-coded latent acoustic features instead of mel-spectrograms resulted in the generated speech sounding normal. Hence, we speculate that there is a difference in local correlation between mel-spectrograms and those neural-coded latent features, leading to convolution being more friendly to modeling the former.

A. Features Analysis

To validate our hypothesis, we visualized the probability distribution of the Pearson correlation coefficients between

adjacent vectors (PCCs-AV) at time and channel axes for different acoustic features. The PCCs-AV are computed according to the following equation:

$$Cor_i = \left| \text{PCCs}(s_i - \mathbb{E}(S), s_{i+1} - \mathbb{E}(S)) \right| \quad (10)$$

where the PCCs denotes the Pearson correlation coefficient function, the s_i is i^{th} feature vector on the time or channel axis, and the $\mathbb{E}(S)$ is the expectation of the feature matrix on the channel or time axis. The subtraction between s_i and $\mathbb{E}(S)$ is used to eliminate redundant information in features. We chose five neural-coded latent features and two signal features for visualization.

Signal Features:

- *Linear*: We extracted 513-dim spectrograms from speech using STFT with a window length of 50ms, a hop length of 12.5ms, and an FFT size of 1024.
- *Mel*: We extracted mel-spectrograms from the linear spectrograms with 80 channels filter between 0 and 8000 Hz.

Neural-coded Latent Features:

- *Encodec & Encodec_VQ*: We employed the pretrained EnCodec [14] released by official implementation⁴ with a bandwidth of 6 kbps to extract the features. The features with $_VQ$ are the indexes of the codebook of EnCodec, and without $_VQ$ are the vectors checked from the codebook according to the indexes.
- *Hificodec & Hificodec_VQ*: We employed the pretrained HiFi-codec [55] released by AcadeMiCodec⁵ to extract the features. The features with $_VQ$ are the indexes of the codebook of HiFi-codec, and without $_VQ$ are the vectors checked from the codebook according to the indexes.
- *VAE*: We trained the VITS [56] cloned from official implementation⁶ with VCTK [57], LibriSpeech [58], CSMSC [59], and Aishell-3 [60], and use its Posterior Encoder to extract 192-dim latent embedding from speech.

We extracted the above features from 400 English utterances and 400 Mandarin utterances. The English audios are randomly selected from VCTK [57], LibriSpeech [58], LJSpeech [61] and Espresso [62]. the Mandarin audios are randomly selected from CSMSC [59] and Aishell-3 [60]. All the audios are resampled to 16K before extracting features, and the silence segments at both ends are excised. It is worth mentioning that the PCCs-AV are counted on the complete speech (including voice phonemes, unvoice phonemes, and non-speech elements such as breathing sound and silence).

The probability distributions of PCCs-AV on the time and channel axes for these two languages are shown in Fig. 3. Since the extraction ways of features are different, the channel axis of signal features contains frequency information. In contrast, the channel axis of neural-coded latent features is disordered and frequency-independent. Comparing the plots in the first row with those in the second row, we find that the PCCs-AV distributions of the same features are similar across

⁴<https://github.com/facebookresearch/encodec>

⁵<https://github.com/yangdongchao/AcadeMiCodec>

⁶<https://github.com/jaywalnut310/vits>

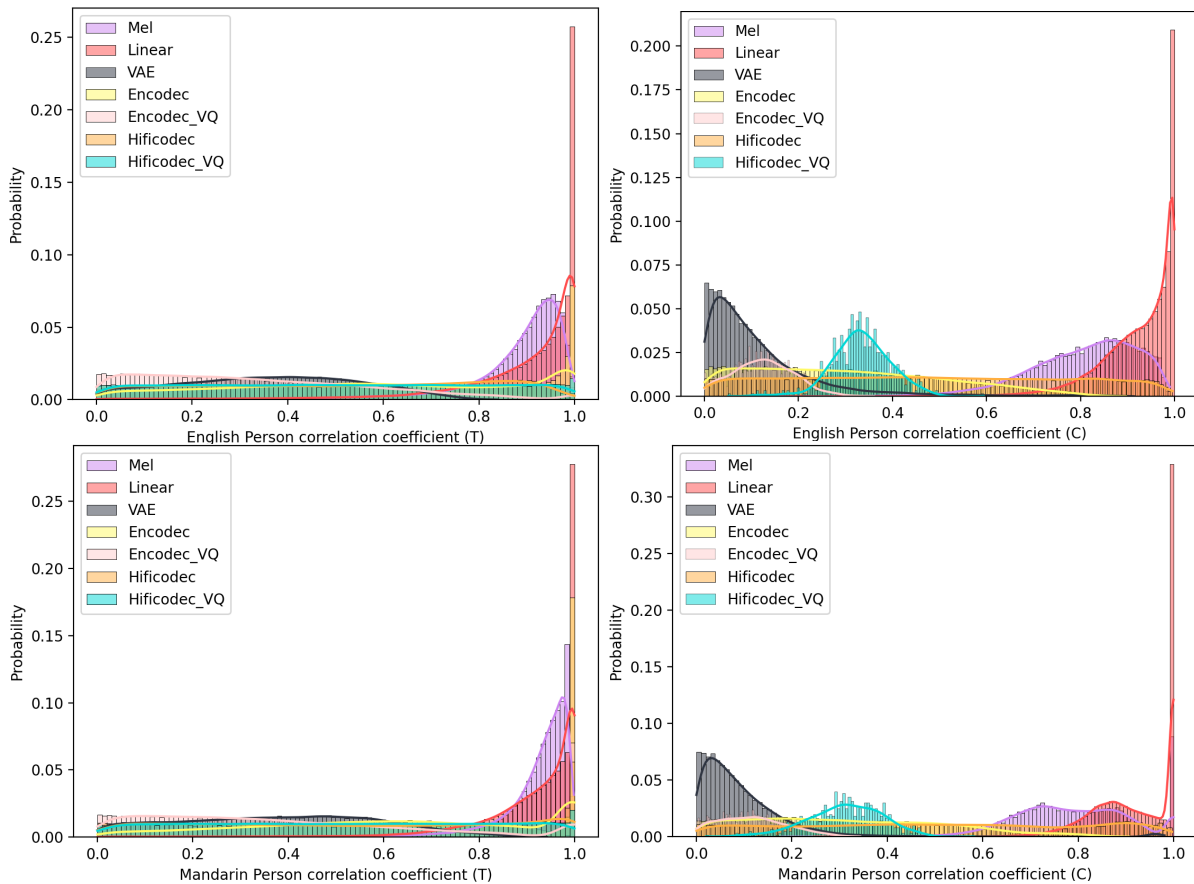


Fig. 3: The probability distribution of the PCCs-AV on time (T) and channel (C) axes for different features in English and Mandarin. PCCs < 0.4 represent weak correlation, $0.4 < \text{PCCs} < 0.6$ represent moderate correlation, and PCCs > 0.6 represent strong correlation.

languages, both in the time and channel axes. Furthermore, the subfigures in the first column show that the PCCs-AV of signal features on the time axis are centrally distributed between 0.8 and 1.0, while the PCCs-AV of neural-coded latent features on the time axis are uniformly distributed between 0-1.0, which suggests that the signal features have significant local correlations in the time domain, whereas the neural-coded latent features do not. This phenomenon can explain why 1D convolution can play a crucial role in modeling mel-spectrograms. In addition, we find that this difference in local correlation is still evident on the channel axis. As shown in the second column of Fig 3, The PCCs-AV of signal features on the channel axis is centrally distributed between 0.6 and 1.0. In contrast, the PCCs-AV of neural-coded latent features on the channel axis are concentrated in a much smaller range.

B. Network Structure

Given that 1D CNN can assist the Transformer in modeling the mel-spectrograms through modeling the strong local correlation on the time axis, we think that the 2D convolution may be better than the 1D convolution for modeling mel-spectrograms since it can restore the local correlation on time and channel axes simultaneously by capturing the information of the surrounding points. To explore the potential advantages of 2D convolution over 1D convolution. We considered two

versions of network structures for the Detail ODE module in SF-Speech, as illustrated in Fig 4. The first version follows the structure in VociBox [23] containing the Transformer with Unet-style link [54] and a 1D convolutional positional embedding layer. The second version uses two 2D depth-wise separable convolution layers to fuse local features of $F_2^{masked} + Prompt$ and H_t' before feeding them into the Transformer. The text feature F_1 does not go through the 2D convolutional layer because its channel axis contains no frequency information. The comparison results of these two network structures can be found in Sec. VI-C.

V. EXPERIMENTS

A. Dataset

As the size of the speech synthesis model increases, the carefully designed data is no longer sufficient for the large synthesis model. Thus, the ability of the synthetic model to utilize wild data becomes more critical. With this in mind, we conduct experiments on MagicData [63], a dataset of Chinese speech recorded through various non-specialized devices. The recorded texts in this dataset cover a variety of daily scenarios, including interactive Q&A, music search, spoken SMS messages, home command control, and so on. The audios in this dataset total 755 hours and are recorded by 1000 speakers

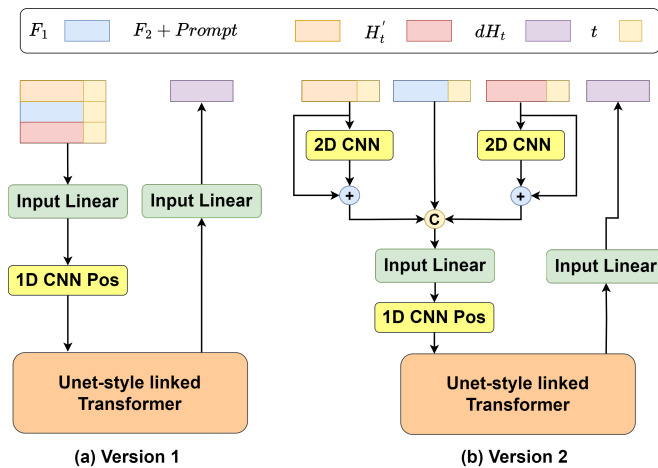


Fig. 4: Two versions of Detail ODE structure. Version 1 consists of the Unet-style linked Transformer and 1D convolutional positional embedding. Version 2 combines 2D convolutional layers based on Version 1.

from different accent regions in China. We divided this corpus into 712.1 hours for training, 14.8 hours for development, and 28.1 hours for testing.

B. Implementation Details

1) *Acoustic Feature*: We employ the mel-spectrograms as the modeling target and a pre-trained BigVGAN⁷ [64] as our vocoder. The mel-spectrogram is computed with an FFT size of 1024, a window length of 1024, a frame length of 256, and 80 channels between 0 and 8000Hz. The recorded texts are converted to phoneme sequences by Phonemizer [65]. We align the phonemes and speech with MFA [66] and cut out the silence at ends according to the align result.

2) *Acoustic Model*: The CNN of the text encoder consists of three 1D convolutional layers with layer normalization, and its LSTM network consists of a Bi-LSTM layer. The hidden dimensions of Bi-LSTM and CNN are 512, and CNN’s kernel size is 5. The LSTM network of the speaker adder also consists of a Bi-LSTM layer with 256 hidden dimensions, while its CNN consists of seven 1D convolutional layers with instance normalization [67]. The kernel size of CNN in the speaker adder is set to 3 and the hidden dimension of the top four layers is set to 512, the middle two layers to 256, and the last to 80. The Unet-style linked Transformer of the Detail ODE containing Attention with linear bias [68] and Root mean square layer normalization [69] has 16 attention heads and an embedding/FFN dimension of 1024/4096, following the VoiceBox [23], but only 8 layers. The 2D CNN in version 2 of Detail ODE has an embedding dimension of 256 and a kernel size of 3×3 . Unless otherwise written, SF-Speech uses the Detail ODE version 1 by default to compare with other ODE-based models under the same network structure.

3) *Training*: We randomly intercepted 648 frames if the audio exceeded this length and continuously masked 70% of

these frames with a random starting point. Only the masked frames are considered when computing the loss. An AdamW optimizer with a peak learning rate of 0.00002, linearly warmed up for 5000 steps and decayed in cosine annealing over the rest steps, was employed to train SF-Speech for 500K iterations.

C. Baselines

Four baseline models are compared in our experiments to evaluate the proposed method on zero-shot voice clone tasks. All baselines are implemented on the MagicData. The implementation details of them are as follows:

- **YourTTS** YourTTS [6] is a classic GSE-based model in zero-shot voice clone tasks. It employed VITS [56] as its backbone and introduced the speaker embedding extracted by H/ASP [70]. We cloned the corrected official implementation⁸ and trained it for 1140K steps with the default configuration.
- **VoiceBox** and **VoiceBox-S** VoiceBox [23] is the SOTA ODE-based zero-shot model. We implemented it and set up two different scales. The first scale follows the 24-layer Transformer in the original paper with 330M parameters. The second scale uses the 8-layer Transformer mentioned in Sec. V-B with 110M parameters called VoiceBox-S. VoiceBox and VoiceBox-S were trained for 500k steps using the same training strategy as SF-Speech. The same BigVGAN was used as their companion vocoder to ensure a fair comparison.
- **VALL-E** VALL-E is the first autoregressive zero-shot voice clone model based on context learning and LLM. We cloned an unofficial implementation⁹ of it and trained it for 600K steps with prefix mode 1 until the valid loss stopped dropping.

D. Evaluation Metrics

We evaluate our model with two aspects: speech quality and timbre similarity. The subjective and objective evaluation metrics for each aspect are as follows:

1) Speech Quality:

- **QMOS** We set a Quality Mean Opinion Score (QMOS) test to evaluate the speech quality. Fifteen native speakers were asked to score between 1 and 5 as the Absolute Category Rating (1: Bad, 2: Poor, 3: Fair, 4: Good, 5: Excellent), and the minimum score interval allowed was 0.5. The final result is presented in the form of a 95% confidence interval.
- **WER** We use the Word Error Rate (WER) of the Automatic Speech Recognition (ASR) system to measure the intelligibility of generated speech as previous works [8], [23]. Given that the speech used for experimentation is Chinese, an open-source WeNet [71] with the pre-trained checkpoint "multi_cn"¹⁰ is used as our ASR system.

⁸<https://github.com/coqui-ai/tts>

⁹<https://github.com/lifeiteng/vall-e>

¹⁰https://github.com/wenet-e2e/wenet/tree/main/examples/multi_cn/s0

⁷https://huggingface.co/nvidia/bigvgan_base_22khz_80band

TABLE I: Subjective and objective evaluation results on ZS-TTS and SR tasks.

Task	Model	Parameters	QMOS	SMOS	WER	SIM-o	SIM-r
	Ground truth		4.07 \pm 0.05	n/a	6.22	n/a	n/a
ZS-TTS	YourTTS	87M	3.09 \pm 0.08	3.52 \pm 0.06	31.66	0.509	n/a
	VALL-E	367M	3.04 \pm 0.10	3.15 \pm 0.09	27.04	0.287	0.336
	VoiceBox-S	110M	3.52 \pm 0.07	3.61 \pm 0.07	15.99	0.516	0.524
	VoiceBox	330M	3.66 \pm 0.05	3.88 \pm 0.07	12.62	0.543	0.554
	Proposed	117M	3.71 \pm 0.04	3.91 \pm 0.05	12.41	0.545	0.554
SR	VoiceBox-S	110M	3.45 \pm 0.06	3.71 \pm 0.10	10.76	0.681	0.714
	VoiceBox	330M	3.69 \pm 0.06	4.00 \pm 0.04	10.68	0.696	0.728
	Proposed	117M	3.73 \pm 0.05	3.97 \pm 0.07	8.69	0.695	0.726

- **DNSMOS** Considering that the quality of the generated speech needs to be repeatedly evaluated many times in Sec. VI-B, we use DNSMOS P. 835 [72] instead of the subjective QMOS to evaluate the speech generated with the different number of function evaluations (NFEs) automatically.

2) Timbre Similarity:

- **SMOS** We set a Similarity Mean Opinion Score (SMOS) test to score the timbre similarity between the prompt and generated speech. The scoring rules are the same as those for QMOS.
- **SIM** We employ ECAPA-TDNN [73], a speaker recognition model, to extract speaker embedding of reference and generated speech. The cosine similarity between two embeddings is used to evaluate the timbre similarity objectively. SIM-o represents the similarity to the original reference audio, and SIM-r reports the similarity to the reconstructed reference audio by the vocoder.

VI. EXPERIMENT RESULTS

A. Zero-shot Voice Clone Evaluation

We compare SP-Speech with the baseline models in two cases: Zero-Shot Text-to-Speech (ZS-TTS) and Speech Restoration (SR). For ZS-TTS tasks, we randomly selected 32 unseen speakers (16 females, 16 males), with 8 utterances per speaker as timbre prompts. One utterance was sampled as the content for each timbre prompt to evaluate subjectively, and 15 utterances for each timbre prompt to evaluate objectively. As for the SR task, we kept 15% of the frames at both ends of the audio and masked the middle 70% to reconstruct. We masked and reconstructed those 256 timbre prompts in TTS tasks for subjective evaluation and sampled 4000 utterances from the test and development sets for objective evaluation. VoiceBox and our model infer speech with an Euler Solver, and the NFEs is set to 8 according to the result of inference efficiency evaluation in Sec. VI-B.

1) ZS-TTS results:

The comparison results between the proposed model and baselines can be found in Tab. I. As it shows, the proposed method achieves the best performance in all the metrics, implying that it has advantages over all the baseline models on the ZS-TTS task.

Focusing on speech quality and intelligibility, we can see that YourTTS and VALL-E perform significantly worse than

those ODE-based models. Even the worst ODE-based model, VoiceBox-S, is 0.43/0.48 higher than YourTTS/VALL-E in QMOS and 15.67%/11.05% lower (drop by nearly half) in WER scores. We found that although both YourTTS and VALL-E are close to each other in QMOS and WER tests, the reasons for their poor performance are different. To fit the training pattern of the LLM model, VALL-E generates speech by modeling discrete acoustic token sequences. However, the correlation between acoustic features after compression and phoneme sequences drops a lot. As a result, 700 hours of training data is not enough to help VALL-E establish a stable mapping between these two sequences, resulting in a gap between the generated speech and the real in spectrograms. In the listening test, we also found that this unstable mapping relationship significantly increased the probability of bad cases (repeated voices, missing words, and total silence or gibberish). These bad cases lead to a large decrease in speech quality and intelligibility. Unlike VALL-E, 700 hours of training data is sufficient for YourTTS, which is based on VITS. Thus, the speech generated by YourTTS has no obvious flaws in the spectrogram, which explains why YourTTS has a higher WER than VALL-E but still gets a higher QMOS than it. We note that the prosody of speech generated by YourTTS significantly differs from real speech, which explains why it performs the worst on WER. We believe this can be attributed to the fact that YourTTS relies only on a global embedding to learn how to model the complex prosody of a speaker with content. When YourTTS is trained on the wild data with a wider distribution of prosody, its generalization to the prosody of unseen speakers deteriorates, leading to unnatural generated speech. On the other hand, in comparison with the ODE-based method, the proposed model has a similar parameters scale to the VoiceBox-S but obtains a reduction of 3.37% on the WER and an increment of 0.19 on the QMOS. Even after increasing the parameters of Voicebox to 330 M (almost triple that of the proposed model), there is still an advantage of the proposed model in terms of QMOS/WER (0.05/0.21%). These results could support our hypothesis about the independent coupling feature of speech in III-B and also proved that independent coupling pairs can significantly improve the performance of the ODE-based model trained with FM.

Turning the perspective to the timbre similarity, we find that the SIM and QMOS of VALL-E are significantly lower than the other models (0.222/0.37 lower than the penulti-

mate YourTTS on SIM-o/SMOS). However, the gap between VALL-E and YourTTS on SIM is more pronounced than on SMOS, with the former being 43.6%, while the latter is only 10.5%. We analyze the reason for this difference in subjective and objective tests: the spectrogram of speech generated by VALLE contains high-frequency horizontal lines, which have little effect on human hearing but are never seen by the speaker recognition model. In addition, YourTTS is competitive in the timbre similarity evaluation, only 0.007 lower on SIM-o and 0.09 lower on the SMOS than the worst ODE-based model. We observed that the speaker consistency fine-tuning employed by YourTTS significantly improved its SIM-o (approximately 0.07). Moreover, the ODE-based methods also show the best performance in timbre similarity evaluation. This result suggests that the context-learning ODE modeling could be the preferred choice for the ZS-TTS task when the training data scale is small. Turning to the comparison among ODE-based models, our proposed model improves 5.2%/5.7%/7.5% on SIM-o/SIM-r/SMOS compared to VoiceBox-S. Even if the parameters number of VoiceBox is increased to 330M, our model can still stay on par with it on SIM-r, SIM-o, and SMOS. These results again demonstrate the significant advantages of the proposed method on the ZS-TTS task.

2) SR results:

Since YourTTS cannot utilize the context of speech and VALL-E can only utilize the left context of the speech, in this section, we only compared SF-Speech, VoiceBox-S, and VoiceBox. As shown at the bottom of Tab I, objective scores in the SR test are higher than those in the ZS-TTS test. This phenomenon is because the speech evaluated in the SR test retained 30% of the audio reconstructed from the real mel-spectrogram. In addition, the proposed models perform different comparative results with baselines regarding speech quality and timbre similarity.

Our model has a significant advantage in the quality evaluation, being 0.28/0.04 higher than VoiceBox-S/VoiceBox on QMOS and 2.07%/2.01% lower on WER, respectively. It is worth noting that VoiceBox does not bring a considerable improvement on WER after tripling the number of parameters. This suggests a possible limitation of VoiceBox in terms of speech intelligibility in this short-time SR task since it directly models the mapping from random noise to mel-spectrogram. However, our model breaks this limitation with a parameter growth of 7M, suggesting that independent coupling between initial data and target data is the key to improving the performance of ODE models trained by FM. Unlike the performance in the speech quality evaluation, when compared to VoiceBox in terms of timbre similarity, the scores of our model suffer from a slight disadvantage, being 0.001/0.002/0.03 lower on SIM-o/SIM-r/SMOS. However, because VoiceBox has 182% more parameters than the proposed model, the scores of the proposed model are still competitive. On the other hand, our model outperforms VoiceBox-S more, improving by 0.014/0.012/0.26 on SIM-o/SIM-r/SMOS. These results again prove the advantages of the proposed method on the SR task.

TABLE II: The RTF and model size of different models on the ZS-TTS task. "RTF1" only considers the inference of the acoustic model, and "RTF2" includes the inference of the vocoder.

Model	Model-Size(M)	RTF1	RTF2
YourTTS	87	0.019	n/a
VALL-E	367	1.884	1.895
VoiceBox	330	0.457	0.590
VoiceBox-S	110	0.105	0.236
Proposed	117	0.120	0.251

B. Inference Efficiency Evaluation

In this section, we first measure the Real-Time Factor (RTF) for different models. Then, we measure objective metrics under different NFEs for ODE-based models and give the optimal NFEs. Finally, we exemplify the speech generated by Voicebox-S and the proposed model under different NFEs to visually present the advantages of the speech generated by our model.

1) RTF results:

We calculate the RTF of different models on ZS-TTS tasks with a 5s reference speech and a Nvidia-V100 GPU. We consider two versions, one computing only the inference of the acoustic model and the other also including the inference of the waveform decoder. All ODE-based models use a NFEs of 8. Since YourTTS is an end-to-end model, it only has RTF results for version 1. As shown in Tab. II, although BigVGAN brings more inference delay than Encodec, RTF1 and RTF2 have the same trend. Therefore, we only analyze RTF1 in detail here. YourTTS is the lightest and the fastest model, with an RTF of 0.019. VoiceBox-S is the second fastest, with an RTF of 0.105, about 5 times that of YourTTS. As an ODE-based model similar to VoiceBox-S, the proposed model obtains an RTF of 0.120, which is only 0.015 more than that of VoiceBox-S, although it has two more modules containing Bi-LSTM. VoiceBox with 330M parameters is the slowest ODE-based model. Although it performs similarly to the proposed model, its RTF is more than 3 times that of SF-Speech. The speed advantage of SF-Speech becomes even more pronounced compared to the autoregressive model, about 16 times faster than VALL-E.

2) NFEs results:

Fig. 5 shows the fluctuation of objective metrics as the NFEs increases. We found that increasing the reverse steps does not always improve the performance of these ODE-based models. We think this is because as the NFEs increases, the ODE-based model adds more audio imperfections (environmental noise, human noise, distortion due to recording devices, etc.) to the generated mel-spectrogram. These imperfections are widely present in the wild data used for training. In addition, different objective metrics have different trends. As the 5 (a) shows, the SIM for these three models have the same trend and peak at NFEs equal to 8. The proposed model outperforms VoiceBox-S in all NFEs cases. Compared with VoiceBox, it shows a slight disadvantage at NFEs less than 8 and is compared favorably at NFEs greater than 8. This

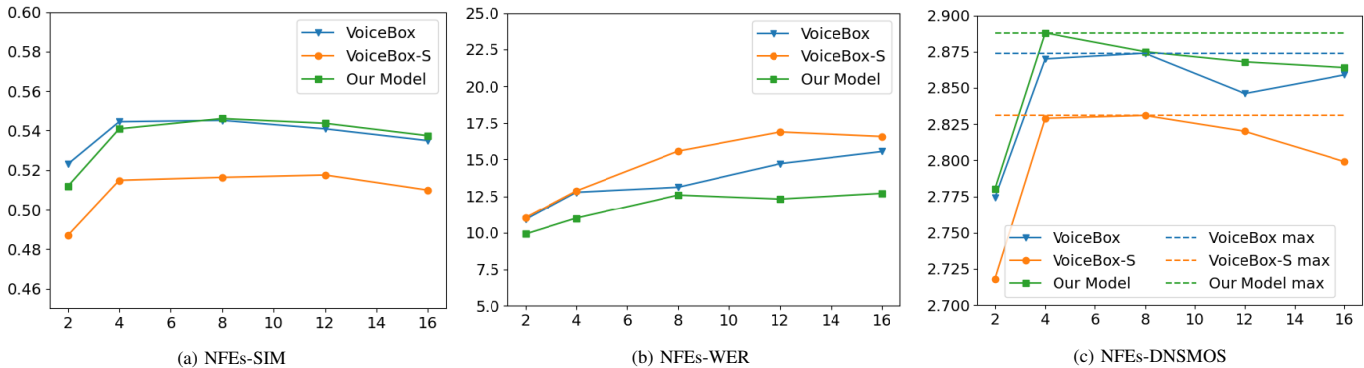


Fig. 5: Objective metrics of generated speech at different NFEs on ZS-TTS task.

result suggests that our approach can mitigate the performance degradation caused by increasing NFEs. On the other hand, as the 5 (b) shows, our model achieves the lowest WER at any NFEs. Unlike the SIM trend, WER keeps deteriorating with increasing NFEs. We believe there is a trade-off between the WER and timbre similarity due to the poor robustness of the ASR model. Our model shows more stable WER than VoiceBox-S and VoiceBox after the NFEs grow to 8, which again proves the superiority of our method. While the lower the NFEs, the lower the WER of the generated speech, we found that when the NFEs is too small, the generated speech sounds unnatural. Because WER does not fully represent the quality of the generated speech, we also tested the DNSMOS for generated speech at different NFEs, as illustrated in Fig. 5 (c). The DNSMOS of VoiceBox and VoiceBox-S peak at NFEs = 8, while the proposed model reaches the peak at NFEs = 4. These results imply that our model can generate higher-quality speech with less than half the parameters of VoiceBox and fewer inference steps. Considering these DNSMOS curves as well as the trade-off between SIM and WER, we decided to set the inference NFEs to 8 for all ODE-based models, although it is not the most beneficial NFEs for SF-Speech.

3) Example analysis:

As shown in Fig. 6, the mel-spectrograms generated by VoiceBox-S and SF-Speech are continuously refined as the NFEs increase. This refinement is mainly reflected in two aspects. On the one hand, as shown in the interior of the blue box, the lines of fundamental frequency and low-frequency harmonics become progressively more apparent with increasing NFE. On the other hand, as shown in the interior of the green box, the high-frequency part of the speech becomes more detailed from a blur. Turning the view to the comparison between different models at the same NFEs, we find that the proposed model draws the fundamental frequency and low-frequency harmonics significantly better than VoiceBox-S, which explains why our model has a clear advantage in the intelligibility of the generated speech. In addition, our model can capture more high-frequency details than VoiceBox-S, as insulated in the green box. It is worth mentioning that VoiceBox-S even destroys this high-frequency detail as NFEs increases, whereas our model avoids this instability by generating mel-spectrograms starting with the coarse features that have basic contours.

TABLE III: Ablation studies on network structure. V1 represents the model using version 1 of Detail ODE, while V2 represents version 2 of Detail ODE.

Task	Model	SIM-o	WER
ZS-TTS	Proposed V1	0.545	12.41
	Proposed V2	0.543	11.46
ZS-SR	Proposed V1	0.692	8.69
	Proposed V2	0.694	8.51

C. Network Comparison

In this section, we evaluated the role of 2D convolution on the tasks ZS-TTS and ZS-SR. The compared results are shown in Tab III. After employing 2D convolution for the fusion of 2D local information of input features on frequency and time axes, the proposed model shows a performance improvement on WER, with a decrease of 0.95% on the ZS-TTS task and 0.18% on the ZS-SR task. However, 2D convolution did not improve speaker similarity, with a SIM-o improvement of 0.002 on the ZS-SR task but a SIM-o decrease of 0.002 on the ZS-TTS task. We think this is because SIM is computed on global speaker embedding extracted from the whole audio, whereas 2D convolution can only assist the proposed model in modeling local information. While the 2D CNN cannot assist the model in speaker similarity, its contribution to speech intelligibility demonstrates that it is helpful for modeling features with high local correlation on time and channel axes. This result implies that designing networks according to the space correlation for different acoustic features is one of the ways to get the most out of these features as possible.

TABLE IV: Ablation studies on training strategy and condition features. F1 and F2 represent the Text Feature and Coarse Feature. M means training masked frames only.

Condition and Strategy	SIM-o	WER
F1+F2+M(proposed)	0.545	12.41
F1+F2	0.531	16.13
F2	0.533	17.94
F1	0.525	17.51

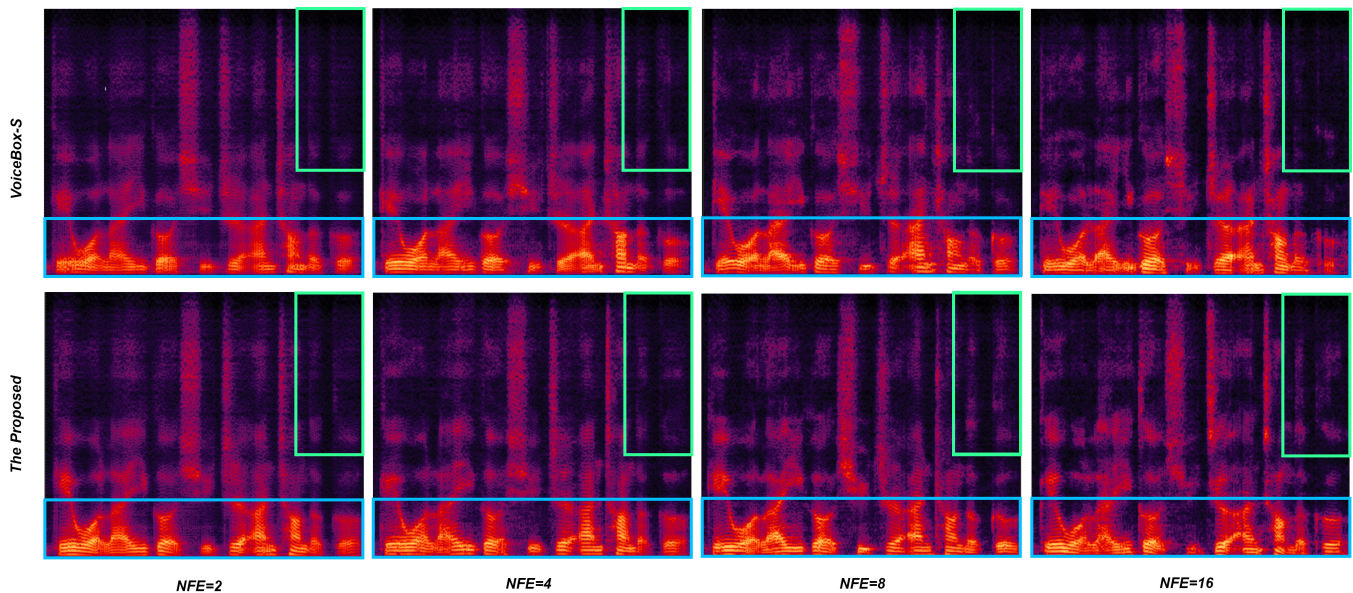


Fig. 6: Mel-spectrograms feature of speech generated by SF-Speech and VoiceBox-S at different NFEs. The proposed model generates speech with clearer low-frequency harmonics (blue box) and more high-frequency details (green box).

D. Ablation Study

In this section, we first tested the effect of training only the masked speech. Then, we ablated the conditional features of the Detail ODE module to verify that the different features contained different information, as we hypothesized in Sec III-B. We trained the SF-Speech containing version 1 of Detail ODE with different training strategies and ODE conditional features to test their performance on the ZS-TTS task. As shown in Tab IV, training only the masked frames significantly improves the timbre similarity and intelligibility of generated speech, with an improvement of 0.014 on SIM-o and a decrease of 3.72% on WER. This result suggests that computing only the loss of masked frames is crucial for these ODE-based models with contextual masking patterns, which is consistent with the previous work [23]. In addition, ablating different conditional features leads to different variations in the SIM-o and WER. When the F1 is removed, the SIM-o increases by 0.002, while the WER increases by 1.81%. This result implies that F1 contains only pronunciation information and text-related prosody. When the F2 is removed, the SIM-o of the generated speech decreases by 0.006, and the WER increases by 1.38%. This result also suggests our hypothesis in Sec. III-B that F2 combines speaker information, the speaker-related prosody, and F1.

VII. CONCLUSION

In this paper, we proposed SF-Speech, a novel ODE-based method for zero-shot voice clone. Specifically, SF-Speech employs a new two-stage method to generate an independently coupled representation of the speech in mel-spectrogram space and utilizes this independently coupled feature to straighten the reverse trajectories learned by the ODE model. Moreover, to explore the relationship between convolution and mel-spectrograms modeling, we visualized

the distribution of Pearson correlation coefficients between adjacent vectors at the time and channel axes for different acoustic features. The experiments conducted on small-scale data of less than 1k hours show that SF-Speech can generate high-quality clone speech with fewer parameters and at a faster speed. Additionally, we investigated the role of 2D convolution in mel-spectrogram modeling compared to 1D convolution within the same framework. The results suggest that designing distinct network structures for different features based on local correlation analysis could be a promising direction for enhancing the quality of generated speech.

However, limited to resources, SF-Speech has not yet been tested on larger-scale parameters and data. We will verify its scalability in future works. In addition, we found that audio imperfections in the wild data degraded the quality of the generated speech, which becomes more pronounced as the number of ODE function evaluations increases. We believe this is because these models based on contextual learning capture not only speaker information but also audio imperfections from the audio context. We will explore the decoupling of speaker information and audio imperfections from the audio context in future research.

REFERENCES

- [1] A. Gibiansky, S. Arik, G. Diamos, J. Miller, K. Peng, W. Ping, J. Raiman, and Y. Zhou, "Deep voice 2: Multi-speaker neural text-to-speech," *Advances in neural information processing systems*, vol. 30, 2017.
- [2] H. B. Moss, V. Aggarwal, N. Prateek, J. González, and R. Barra-Chicote, "Boffin tts: Few-shot speaker adaptation by bayesian optimization," in *ICASSP 2020-2020 IEEE International Conference on Acoustics, Speech and Signal Processing (ICASSP)*. IEEE, 2020, pp. 7639–7643.
- [3] S.-F. Huang, C.-J. Lin, D.-R. Liu, Y.-C. Chen, and H.-y. Lee, "Meta-tts: Meta-learning for few-shot speaker adaptive text-to-speech," *IEEE/ACM Transactions on Audio, Speech, and Language Processing*, vol. 30, pp. 1558–1571, 2022.
- [4] D. Min, D. B. Lee, E. Yang, and S. J. Hwang, "Meta-stylespeech: Multi-speaker adaptive text-to-speech generation," in *International Conference on Machine Learning*. PMLR, 2021, pp. 7748–7759.

- [5] Z. Jiang, Y. Ren, Z. Ye, J. Liu, C. Zhang, Q. Yang, S. Ji, R. Huang, C. Wang, X. Yin *et al.*, “Mega-tts: Zero-shot text-to-speech at scale with intrinsic inductive bias,” *arXiv preprint arXiv:2306.03509*, 2023.
- [6] E. Casanova, J. Weber, C. D. Shulby, A. C. Junior, E. Gölge, and M. A. Ponti, “Yourtts: Towards zero-shot multi-speaker tts and zero-shot voice conversion for everyone,” in *International Conference on Machine Learning*. PMLR, 2022, pp. 2709–2720.
- [7] J. Li, W. Tu, and L. Xiao, “Freevc: Towards high-quality text-free one-shot voice conversion,” in *ICASSP 2023-2023 IEEE International Conference on Acoustics, Speech and Signal Processing (ICASSP)*. IEEE, 2023, pp. 1–5.
- [8] C. Wang, S. Chen, Y. Wu, Z. Zhang, L. Zhou, S. Liu, Z. Chen, Y. Liu, H. Wang, J. Li *et al.*, “Neural codec language models are zero-shot text to speech synthesizers,” *arXiv preprint arXiv:2301.02111*, 2023.
- [9] D. Yang, J. Tian, X. Tan, R. Huang, S. Liu, X. Chang, J. Shi, S. Zhao, J. Bian, X. Wu *et al.*, “Uniaudio: An audio foundation model toward universal audio generation,” *arXiv preprint arXiv:2310.00704*, 2023.
- [10] E. Casanova, K. Davis, E. Gölge, G. Gökner, I. Gulea, L. Hart, A. Aljafari, J. Meyer, R. Morais, S. Olayemi *et al.*, “Xtts: a massively multilingual zero-shot text-to-speech model,” *arXiv e-prints*, pp. arXiv–2406, 2024.
- [11] L. Floridi and M. Chiriatti, “Gpt-3: Its nature, scope, limits, and consequences,” *Minds and Machines*, vol. 30, pp. 681–694, 2020.
- [12] H. Touvron, T. Lavril, G. Izacard, X. Martinet, M.-A. Lachaux, T. Lacroix, B. Rozière, N. Goyal, E. Hambro, F. Azhar *et al.*, “Llama: Open and efficient foundation language models,” *arXiv preprint arXiv:2302.13971*, 2023.
- [13] N. Zeghidour, A. Luebs, A. Omran, J. Skoglund, and M. Tagliasacchi, “Soundstream: An end-to-end neural audio codec,” *IEEE/ACM Transactions on Audio, Speech, and Language Processing*, vol. 30, pp. 495–507, 2021.
- [14] A. Défossez, J. Copet, G. Synnaeve, and Y. Adi, “High fidelity neural audio compression,” *arXiv preprint arXiv:2210.13438*, 2022.
- [15] R. Kumar, P. Seetharaman, A. Luebs, I. Kumar, and K. Kumar, “High-fidelity audio compression with improved rvqgan,” *Advances in Neural Information Processing Systems*, vol. 36, 2024.
- [16] Z. Ju, Y. Wang, K. Shen, X. Tan, D. Xin, D. Yang, Y. Liu, Y. Leng, K. Song, S. Tang *et al.*, “Autoregressive speech synthesis without vector quantization,” *arXiv preprint arXiv:2403.03100*, 2024.
- [17] J. Austin, D. D. Johnson, J. Ho, D. Tarlow, and R. Van Den Berg, “Structured denoising diffusion models in discrete state-spaces,” *Advances in Neural Information Processing Systems*, vol. 34, pp. 17981–17993, 2021.
- [18] M. Łajszczak, G. Cámara, Y. Li, F. Beyhan, A. van Korlaar, F. Yang, A. Joly, Á. Martín-Cortinas, A. Abbas, A. Michalski *et al.*, “Base tts: Lessons from building a billion-parameter text-to-speech model on 100k hours of data,” *arXiv preprint arXiv:2402.08093*, 2024.
- [19] L. Meng, L. Zhou, S. Liu, S. Chen, B. Han, S. Hu, Y. Liu, J. Li, S. Zhao, X. Wu *et al.*, “Autoregressive speech synthesis without vector quantization,” *arXiv preprint arXiv:2407.08551*, 2024.
- [20] S. Wang and É. Székely, “Evaluating text-to-speech synthesis from a large discrete token-based speech language model,” *arXiv preprint arXiv:2405.09768*, 2024.
- [21] C. Qiang, H. Li, Y. Tian, Y. Zhao, Y. Zhang, L. Wang, and J. Dang, “High-fidelity speech synthesis with minimal supervision: All using diffusion models,” in *ICASSP 2024-2024 IEEE International Conference on Acoustics, Speech and Signal Processing (ICASSP)*. IEEE, 2024, pp. 10781–10785.
- [22] K. Shen, Z. Ju, X. Tan, Y. Liu, Y. Leng, L. He, T. Qin, S. Zhao, and J. Bian, “Naturalspeech 2: Latent diffusion models are natural and zero-shot speech and singing synthesizers,” *arXiv preprint arXiv:2304.09116*, 2023.
- [23] M. Le, A. Vyas, B. Shi, B. Karrer, L. Sari, R. Moritz, M. Williamson, V. Manohar, Y. Adi, J. Mahadeokar *et al.*, “Voicebox: Text-guided multilingual universal speech generation at scale,” *arXiv preprint arXiv:2306.15687*, 2023.
- [24] S. Kim, K. Shih, J. F. Santos, E. Bakhturina, M. Desta, R. Valle, S. Yoon, B. Catanzaro *et al.*, “P-flow: A fast and data-efficient zero-shot tts through speech prompting,” *Advances in Neural Information Processing Systems*, vol. 36, 2024.
- [25] R. T. Chen, Y. Rubanova, J. Bettencourt, and D. K. Duvenaud, “Neural ordinary differential equations,” *Advances in neural information processing systems*, vol. 31, 2018.
- [26] Y. Lipman, R. T. Chen, H. Ben-Hamu, M. Nickel, and M. Le, “Flow matching for generative modeling,” *arXiv preprint arXiv:2210.02747*, 2022.
- [27] S. Lee, B. Kim, and J. C. Ye, “Minimizing trajectory curvature of ode-based generative models,” in *International Conference on Machine Learning*. PMLR, 2023, pp. 18957–18973.
- [28] X. Liu, C. Gong, and Q. Liu, “Flow straight and fast: Learning to generate and transfer data with rectified flow,” *arXiv preprint arXiv:2209.03003*, 2022.
- [29] Y. Ren, Y. Ruan, X. Tan, T. Qin, S. Zhao, Z. Zhao, and T.-Y. Liu, “Fastspeech: Fast, robust and controllable text to speech,” *Advances in neural information processing systems*, vol. 32, 2019.
- [30] Y. Ren, C. Hu, X. Tan, T. Qin, S. Zhao, Z. Zhao, and T.-Y. Liu, “Fastspeech 2: Fast and high-quality end-to-end text to speech,” *arXiv preprint arXiv:2006.04558*, 2020.
- [31] Y. Liu, Z. Xu, G. Wang, K. Chen, B. Li, X. Tan, J. Li, L. He, and S. Zhao, “Delightfultts: The microsoft speech synthesis system for blizzard challenge 2021,” *arXiv preprint arXiv:2110.12612*, 2021.
- [32] Y. A. Li, C. Han, and N. Mesgarani, “Styletts: A style-based generative model for natural and diverse text-to-speech synthesis,” *arXiv preprint arXiv:2205.15439*, 2022.
- [33] Y. Song, J. Sohl-Dickstein, D. P. Kingma, A. Kumar, S. Ermon, and B. Poole, “Score-based generative modeling through stochastic differential equations,” *arXiv preprint arXiv:2011.13456*, 2020.
- [34] A. Hyvärinen and P. Dayan, “Estimation of non-normalized statistical models by score matching,” *Journal of Machine Learning Research*, vol. 6, no. 4, 2005.
- [35] R. Rombach, A. Blattmann, D. Lorenz, P. Esser, and B. Ommer, “High-resolution image synthesis with latent diffusion models,” in *Proceedings of the IEEE/CVF conference on computer vision and pattern recognition*, 2022, pp. 10684–10695.
- [36] A. Ramesh, P. Dhariwal, A. Nichol, C. Chu, and M. Chen, “Hierarchical text-conditional image generation with clip latents,” *arXiv preprint arXiv:2204.06125*, vol. 1, no. 2, p. 3, 2022.
- [37] Z. Kong, W. Ping, J. Huang, K. Zhao, and B. Catanzaro, “Dif-fwave: A versatile diffusion model for audio synthesis,” *arXiv preprint arXiv:2009.09761*, 2020.
- [38] N. Chen, Y. Zhang, H. Zen, R. J. Weiss, M. Norouzi, and W. Chan, “Wavegrad: Estimating gradients for waveform generation,” *arXiv preprint arXiv:2009.00713*, 2020.
- [39] Y. Koizumi, H. Zen, K. Yatabe, N. Chen, and M. Bacchiani, “Specgrad: Diffusion probabilistic model based neural vocoder with adaptive noise spectral shaping,” *arXiv preprint arXiv:2203.16749*, 2022.
- [40] V. Popov, I. Vovk, V. Gogoryan, T. Sadekova, and M. Kudinov, “Grad-tts: A diffusion probabilistic model for text-to-speech,” in *International Conference on Machine Learning*. PMLR, 2021, pp. 8599–8608.
- [41] X. Jing, Y. Chang, Z. Yang, J. Xie, A. Triantafyllopoulos, and B. W. Schuller, “U-dit tts: U-diffusion vision transformer for text-to-speech,” in *Speech Communication; 15th ITG Conference*. VDE, 2023, pp. 56–60.
- [42] H. Zheng, P. He, W. Chen, and M. Zhou, “Truncated diffusion probabilistic models,” *arXiv preprint arXiv:2202.09671*, vol. 1, no. 3, pp. 1–2, 2022.
- [43] Z. Lyu, X. Xu, C. Yang, D. Lin, and B. Dai, “Accelerating diffusion models via early stop of the diffusion process,” *arXiv preprint arXiv:2205.12524*, 2022.
- [44] Z. Kong and W. Ping, “On fast sampling of diffusion probabilistic models,” *arXiv preprint arXiv:2106.00132*, 2021.
- [45] C. Lu, Y. Zhou, F. Bao, J. Chen, C. Li, and J. Zhu, “Dpm-solver: A fast ode solver for diffusion probabilistic model sampling in around 10 steps,” *Advances in Neural Information Processing Systems*, vol. 35, pp. 5775–5787, 2022.
- [46] Y. Sun, J. Yang, and W. Zhao, “Ito-taylor schemes for solving mean-field stochastic differential equations,” *Numerical Mathematics: Theory, Methods and Applications*, vol. 10, no. 4, pp. 798–828, 2017.
- [47] S. Mehta, R. Tu, J. Beskow, É. Székely, and G. E. Henter, “Matcha-tts: A fast tts architecture with conditional flow matching,” in *ICASSP 2024-2024 IEEE International Conference on Acoustics, Speech and Signal Processing (ICASSP)*. IEEE, 2024, pp. 11341–11345.
- [48] Y. Guo, C. Du, Z. Ma, X. Chen, and K. Yu, “Voiceflow: Efficient text-to-speech with rectified flow matching,” in *ICASSP 2024-2024 IEEE International Conference on Acoustics, Speech and Signal Processing (ICASSP)*. IEEE, 2024, pp. 11121–11125.
- [49] I. Higgins, L. Matthey, A. Pal, C. Burgess, X. Glorot, M. Botvinick, S. Mohamed, and A. Lerchner, “beta-vae: Learning basic visual concepts with a constrained variational framework,” in *International conference on learning representations*, 2016.
- [50] A. Vaswani, N. Shazeer, N. Parmar, J. Uszkoreit, L. Jones, A. N. Gomez, E. Kaiser, and I. Polosukhin, “Attention is all you need,” *Advances in neural information processing systems*, vol. 30, 2017.

- [51] A. Gulati, J. Qin, C.-C. Chiu, N. Parmar, Y. Zhang, J. Yu, W. Han, S. Wang, Z. Zhang, Y. Wu *et al.*, “Conformer: Convolution-augmented transformer for speech recognition,” *arXiv preprint arXiv:2005.08100*, 2020.
- [52] J. Ho, A. Jain, and P. Abbeel, “Denoising diffusion probabilistic models,” *Advances in neural information processing systems*, vol. 33, pp. 6840–6851, 2020.
- [53] W. Peebles and S. Xie, “Scalable diffusion models with transformers,” in *Proceedings of the IEEE/CVF International Conference on Computer Vision, 2023*, pp. 4195–4205.
- [54] F. Bao, S. Nie, K. Xue, Y. Cao, C. Li, H. Su, and J. Zhu, “All are worth words: A vit backbone for diffusion models,” in *Proceedings of the IEEE/CVF conference on computer vision and pattern recognition, 2023*, pp. 22 669–22 679.
- [55] D. Yang, S. Liu, R. Huang, J. Tian, C. Weng, and Y. Zou, “Hifi-codec: Group-residual vector quantization for high fidelity audio codec,” *arXiv preprint arXiv:2305.02765*, 2023.
- [56] J. Kim, J. Kong, and J. Son, “Conditional variational autoencoder with adversarial learning for end-to-end text-to-speech,” in *International Conference on Machine Learning*. PMLR, 2021, pp. 5530–5540.
- [57] C. Veaux, J. Yamagishi, and K. MacDonald, “Cstr vctk corpus: English multi-speaker corpus for cstr voice cloning toolkit,” 2017.
- [58] V. Panayotov, G. Chen, D. Povey, and S. Khudanpur, “Librispeech: an asr corpus based on public domain audio books,” in *2015 IEEE international conference on acoustics, speech and signal processing (ICASSP)*. IEEE, 2015, pp. 5206–5210.
- [59] D. Baker, “Chinese standard mandarin speech corpus,” <https://www.data-baker.com/opensource.html>, 2017.
- [60] Y. Shi, H. Bu, X. Xu, S. Zhang, and M. Li, “AISHELL-3: A Multi-Speaker Mandarin TTS Corpus,” in *Proc. Interspeech 2021*, 2021, pp. 2756–2760.
- [61] K. Ito and L. Johnson, “The lj speech dataset,” <https://keithito.com/LJ-Speech-Dataset/>, 2017.
- [62] T. A. Nguyen, W.-N. Hsu, A. d’Avirro, B. Shi, I. Gat, M. Fazel-Zarani, T. Remez, J. Copet, G. Synnaeve, M. Hassid *et al.*, “Expresso: A benchmark and analysis of discrete expressive speech resynthesis,” *arXiv preprint arXiv:2308.05725*, 2023.
- [63] L. Magic Data Technology Co., “Magicdata mandarin chinese read speech corpus,” <https://www.openslr.org/68/>, 2019.
- [64] S.-g. Lee, W. Ping, B. Ginsburg, B. Catanzaro, and S. Yoon, “Bigvgan: A universal neural vocoder with large-scale training,” *arXiv preprint arXiv:2206.04658*, 2022.
- [65] M. Bernard and H. Titeux, “Phonemizer: Text to phones transcription for multiple languages in python,” *Journal of Open Source Software*, vol. 6, no. 68, p. 3958, 2021. [Online]. Available: <https://doi.org/10.21105/joss.03958>
- [66] M. McAuliffe, M. Socolof, S. Mihuc, M. Wagner, and M. Sonderegger, “Montreal forced aligner: Trainable text-speech alignment using kaldii,” in *Interspeech*, 2017, pp. 498–502.
- [67] D. Ulyanov, A. Vedaldi, and V. Lempitsky, “Instance normalization: The missing ingredient for fast stylization,” *arXiv preprint arXiv:1607.08022*, 2016.
- [68] O. Press, N. A. Smith, and M. Lewis, “Train short, test long: Attention with linear biases enables input length extrapolation,” *arXiv preprint arXiv:2108.12409*, 2021.
- [69] B. Zhang and R. Sennrich, “Root mean square layer normalization,” *Advances in Neural Information Processing Systems*, vol. 32, 2019.
- [70] H. S. Heo, B.-J. Lee, J. Huh, and J. S. Chung, “Clova baseline system for the voxceleb speaker recognition challenge 2020,” *arXiv preprint arXiv:2009.14153*, 2020.
- [71] B. Zhang, D. Wu, Z. Peng, X. Song, Z. Yao, H. Lv, L. Xie, C. Yang, F. Pan, and J. Niu, “Wenet 2.0: More productive end-to-end speech recognition toolkit,” *arXiv preprint arXiv:2203.15455*, 2022.
- [72] C. K. Reddy, V. Gopal, and R. Cutler, “Dnsmos p. 835: A non-intrusive perceptual objective speech quality metric to evaluate noise suppressors,” in *ICASSP 2022-2022 IEEE International Conference on Acoustics, Speech and Signal Processing (ICASSP)*. IEEE, 2022, pp. 886–890.
- [73] B. Desplanques, J. Thienpondt, and K. Demuynck, “Ecapa-tdnn: Emphasized channel attention, propagation and aggregation in tdnn based speaker verification,” *arXiv preprint arXiv:2005.07143*, 2020.